

Department of Social Systems and Management

Discussion Paper Series

No. 1149

**Numerical Evaluation of Dynamic Behavior of
Ornstein-Uhlenbeck Processes Modified by
Various Boundaries and Its Application to
Pricing Barrier Options**

by

Jun-ya Gotoh, Hui Jin, and Ushio Sumita

June 2006

UNIVERSITY OF TSUKUBA
Tsukuba, Ibaraki 305-8573
JAPAN

NUMERICAL EVALUAION OF DYNAMIC BEHAVIOR OF ORNSTEIN-UHLENBECK PROCESSES MODIFIED BY VARIOUS BOUNDARIES AND ITS APPLICATION TO PRICING BARRIER OPTIONS

e-mail address for contact: `jgoto@sk.tsukuba.ac.jp` (Jun-ya Gotoh)

Short Title: *Evaluation of Dynamic Behavior of Modified O-U Processes*

Jun-ya GOTOH Graduate School of Systems and Information Engineering,
University of Tsukuba,
1-1-1 Tennoudai, Tsukuba-City, Ibaraki 305-8573, Japan
e-mail : `jgoto@sk.tsukuba.ac.jp`

Hui JIN Graduate School of Systems and Information Engineering,
University of Tsukuba,
e-mail : `kinki@sk.tsukuba.ac.jp`

Ushio SUMITA Graduate School of Systems and Information Engineering,
University of Tsukuba,
e-mail : `sumita@sk.tsukuba.ac.jp`

Abstract

In financial engineering, one often encounters barrier options in which an action promised in the contract is taken if the underlying asset value becomes too high or too low. In order to compute the corresponding prices, it is necessary to capture dynamic behavior of the associated stochastic process modified by boundaries. To the best knowledge of the authors, there is no algorithmic approach available to compute such prices repeatedly in a systematic manner. The purpose of this paper is to develop computational algorithms to capture the dynamic behavior of Ornstein-Uhlenbeck processes modified by various boundaries based on the Ehrenfest approximation approach established in Sumita, Gotoh and Jin[4]. As an application, we evaluate the prices of up-and-out call options maturing at time τ_M with strike price K_S written on a discount bond maturing at time T , demonstrating the usefulness, speed and accuracy of the proposed computational algorithms.

Keywords : Prices of barrier options, Modified Ornstein-Uhlenbeck (O-U) process, Absorbing boundaries, Replacement boundaries, Reflection boundaries, Uniformization procedure

0 Introduction

The Ornstein-Uhlenbeck (O-U) process $\{X_{\text{OU}}(t) : t \geq 0\}$ on \mathbb{R} is a Markov diffusion process whose probability density function $f(x, t) := \frac{d}{dx} P\{X_{\text{OU}}(t) \leq x\}$ is governed by the forward diffusion equation

$$\frac{\partial}{\partial t} f(x, t) = \frac{\partial^2}{\partial x^2} f(x, t) + \frac{\partial}{\partial x} [x f(x, t)]. \quad (0.1)$$

Since this process is of practical importance, it has been widely studied and applied to modeling many real dynamics. Recently the usefulness of the O-U process has been reinforced in the area of financial engineering, where spot interest rates are represented by O-U processes.

More specifically, let us consider a one factor term structure model $\{\widehat{X}_{\text{OU}}(t) : t \geq 0\}$ characterized by a stochastic differential equation of the form

$$d\widehat{X}_{\text{OU}}(t) = (\phi - \alpha \widehat{X}_{\text{OU}}(t))dt + \sigma dW(t), \quad (0.2)$$

where $\widehat{X}_{\text{OU}}(t)$ is a random short rate, $W(t)$ is the standard Wiener process, ϕ is a mean reversion level, $\alpha > 0$ is a reversion speed and $\sigma > 0$ is a volatility factor. This model is called the Vasicek model, see e.g., [5]. If we define $\{\widetilde{X}_{\text{OU}}(t) : t \geq 0\}$ by

$$\widetilde{X}_{\text{OU}}(t) := \frac{\sigma}{\sqrt{2\alpha}} X_{\text{OU}}(\alpha t), \quad (0.3)$$

one finds, after a little algebra, that

$$\widehat{X}_{\text{OU}}(t) = \widetilde{X}_{\text{OU}}(t) + \theta(t), \quad (0.4)$$

where $\widetilde{X}_{\text{OU}}(0) = 0$ and

$$\theta(t) \stackrel{\text{def}}{=} \frac{\phi}{\alpha} (1 - e^{-\alpha t}) + \widehat{X}_{\text{OU}}(0) e^{-\alpha t}. \quad (0.5)$$

We now consider an up-and-out call option maturing at time τ_{M} with strike price K_{S} , where the option is written on a discount bond of maturity at time T with maturity value

of one. This option is nullified and is of zero value if $\widehat{X}_{OU}(t)$ exceeds the prespecified upper limit r_B before τ_M . Otherwise, it has the value at τ_M determined in the following manner. Let $D(\tau|\hat{x}_0, T)$ be the price of the discount bond at time τ given $\widehat{X}_{OU}(0) = \hat{x}_0$. Then the price of the up-and-out call option at time τ_M , denoted by $\pi_{KO}(\tau_M|\hat{x}_0, T)$, can be expressed in terms of the first passage time $T_{\hat{x}_0 r_B} = \inf \{t : \widehat{X}_{OU}(t) > r_B | \widehat{X}_{OU}(0) = \hat{x}_0\}$ as

$$\pi_{KO}(\tau_M|\hat{x}_0, T) = E \left[\{D(\tau_M|\hat{x}_0, T) - K_S\}^+ 1_{\{T_{\hat{x}_0 r_B} > \tau_M\}} \right], \quad (0.6)$$

where $\{a\}^+ = \max\{a, 0\}$ and

$$1_{\{A\}} = \begin{cases} 1, & \text{if } A \text{ is true,} \\ 0, & \text{if } A \text{ is false.} \end{cases} \quad (0.7)$$

The strike price K_S may be given by

$$K_S = e^{-r_S(T-\tau_M)}, \quad (0.8)$$

where the value of the discount bond is depreciated at time τ_M by a prespecified rate r_S .

Evaluating $\pi_{KO}(\tau_M|\hat{x}_0, T)$ requires the joint distribution of $P \left[\widehat{X}_{OU}(t) \leq x, T_{\hat{x}_0 r_B} > \tau_M | \widehat{X}_{OU}(0) = \hat{x}_0 \right]$. In addition, the joint distribution has to be computed repeatedly with speed and accuracy for different values of the underlying parameters. To the authors' best knowledge, there exist no systematic algorithms to overcome this difficulty in the literature. The computational algorithms proposed in this paper provide a powerful numerical vehicle for filling this gap.

The purpose of this paper is to develop computational algorithms for capturing the dynamic behavior of the O-U process $\{X_{OU}(t) : t \geq 0\}$ modified by various boundaries. Despite the underlying simplicity associated with the Gaussian transition structure, the dynamic behavior of the O-U process with such boundaries becomes analytically intractable. Typical boundaries include absorbing boundaries, replacement boundaries, and reflection boundaries which are special cases of replacement boundaries. The reader is referred to Feller [1] for further details. Figure 0.1(a) depicts the modified O-U process with one absorbing boundary. The modified O-U process with two absorbing boundaries is illustrated in Figure 0.1(b). When the upper and lower boundaries are symmetric about 0, this process expresses the first passage time of $|X_{OU}(t)|$. Additional cases for replacement and reflection boundaries are shown in Figures 0.1(c) and 0.1(d), respectively. These boundaries play an important

role in dealing with a variety of financial derivatives. The value of up-and-out call option in (0.6), for example, can be evaluated by dealing with an absorbing boundary combined with appropriate shifting and scaling operations specified in (0.3) and (0.4).

[Figure 0.1]

In the previous paper by the authors [4], it is shown, through the spectral analysis of a birth-death process, that a sequence of Ehrenfest processes with appropriate scaling and shifting converges in law to the O-U process $\{X_{OU}(t) : t \geq 0\}$. The corresponding first passage times and the historical maximum also converge in law to those of $\{X_{OU}(t) : t \geq 0\}$. It is worth noting that this approach approximates the O-U process by discretizing only the state space, not the time axis. More specifically, a finite range of $\{X_{OU}(t) : t \geq 0\}$ is represented by $2V + 1$ discrete states where V is a positive integer. Then the O-U process $\{X_{OU}(t) : t \geq 0\}$ is approximated by $\{X_V(t) : t \geq 0\}$ which is constructed from the underlying Ehrenfest process defined on $\mathcal{N}_V = \{0, 1, \dots, 2V\}$ with appropriate scaling and shifting. The zero points of the orthogonal polynomials associated with the spectral representation of the Ehrenfest process are then computed, enabling one to evaluate the distributions of the first passage times and the historical maximum.

Additional numerical experiments following the previous paper [4] have revealed that some zero points tend to cluster near the ends of \mathcal{N}_V with diminishing distances among themselves. Consequently, those clustering zeros cannot be computed with accuracy for $V > 100$. For example, with $V = 100$, only three digit accuracy is assured for the survival functions of the first passage times. In order to overcome this numerical difficulty, we propose an alternative approach based on the uniformization procedure of Keilson [3]. As we will see, the uniformization procedure is numerically stable with speed and accuracy, enabling one to cope with $V = 20,000$ or more where the computational burden increases only as a linear function of V . Based on this approach, the modified Ehrenfest processes with different boundaries are evaluated, which in turn captures the dynamic behavior of the modified O-U processes with corresponding boundaries. The proposed approach enables one to evaluate prices of a variety of barrier options as represented by (0.6) with speed and accuracy.

The structure of this paper is as follows. In Section 1, the key results of [4] relevant to this paper are reviewed succinctly. The uniformization procedure of Keilson [3] for temporally homogeneous Markov chains in continuous time is summarized in Section 2, together with algorithms for evaluating the distributions of associated first passage times and the historical maximum. Sections 3, 4, and 5 deal with the modified O-U process with one absorbing boundary, two absorbing boundaries, and replacement and reflection boundaries, respectively. Numerical results are also presented, demonstrating the convergence of the modified Ehrenfest process as $V \rightarrow \infty$ with speed and accuracy. In Section 6, the price of the up-and-out call option of (0.6) is evaluated explicitly. For comparison purpose, we also develop a modified Hull-White trinomial tree approach to deal with absorbing boundaries. While the modified Hull-White trinomial tree approach cannot be employed for certain parameter values, the proposed Ehrenfest approach can cope with any parameter values with speed and accuracy. Because of this, in mechanizing the entire computational procedures for repeated evaluations under different parameter values, the proposed Ehrenfest approach is much superior to the modified Hull-White trinomial tree approach.

For notational convenience, throughout the paper, we denote a vector by attaching single underline as \underline{x} , and a matrix by attaching double underlines as $\underline{\underline{a}}$. Moreover, $\underline{1}$ and $\underline{0}$ mean vectors whose all elements are 1 and 0, respectively. The vector \underline{u}_m means that its element corresponding to state m is 1 and all other elements are 0. For an $N \times N$ matrix $\underline{\underline{a}}$, a submatrix on $G \subset \{1, \dots, N\}$ for rows and on $B \subset \{1, \dots, N\}$ for columns is denoted by $\underline{\underline{a}}_{GB} = [a_{ij}]_{i \in G, j \in B}$.

1 Convergence of Ehrenfest Process to O-U Process and Corresponding State Conversion

We consider a birth-death process $\{N_{2V}(t) : t \geq 0\}$ on $\mathcal{N}_V = \{0, 1, \dots, 2V\}$ governed by upward and downward transition rates given respectively by

$$\lambda_m = V - \frac{m}{2} \quad \text{and} \quad \mu_m = \frac{m}{2}, \quad m \in \mathcal{N}_V. \quad (1.1)$$

This Markov chain is called an Ehrenfest process in continuous time. From Eq.(1.1), one sees that the local growth rate of the variance is given by

$$\nu_m := \lambda_m + \mu_m = V, \quad m \in \mathcal{N}_V, \quad (1.2)$$

which is independent of m , and the local velocity is given by

$$\lambda_m - \mu_m = V - m. \quad (1.3)$$

For the associated stationary chain $\{N_{VS}(t) : t \geq 0\}$, one has

$$\text{cov}[N_{VS}(t), N_{VS}(t + \tau)] = \frac{V}{4} e^{-\tau}, \quad (1.4)$$

and asymptotic normality. The O-U process is characterized by its Markov property, normal distribution, and exponential covariance function. Because of the properties of the Ehrenfest process specified in Eqs.(1.1) through (1.4) together with its asymptotic normality, one expects that a sequence of processes $\{X_V(t) : t \geq 0\}$, $V = 1, 2, 3, \dots$, defined by

$$X_V(t) = \sqrt{\frac{2}{V}} N_{2V}(t) - \sqrt{2V} \quad (1.5)$$

converges in law to the O-U process as $V \rightarrow \infty$. Indeed, this is formally proven in [4].

We note that $\{X_V(t) : t \geq 0\}$ has discrete support defined by

$$r(m) := \sqrt{\frac{2}{V}} m - \sqrt{2V}, \quad m = 0, 1, \dots, 2V. \quad (1.6)$$

The correspondence between the states of $N_V(t)$ and those of $X_V(t)$ is summarized in Table 1.1, where

$$\eta_V(x) := \left\lceil \sqrt{\frac{V}{2}} x \right\rceil. \quad (1.7)$$

[Table 1.1]

The following two theorems of [4] are relevant to this paper. For the O-U process $\{X_{OU}(t) : t \geq 0\}$, its initial state is denoted by $X_{OU}(0) = x_0$.

Theorem 1.1 ([4]) *For any $x_0, x \in \mathbb{R}$, let $m := V + \eta_V(x_0)$ and $n := V + \eta_V(x)$. Let $T_V(m, n) := \inf \{t : X_V(t) = r(n) | X_V(0) = r(m)\}$ and $T_{OU}(x_0, x) := \inf \{t : X_{OU}(t) = x | X_{OU}(0) = x_0\}$. Then, $T_V(m, n)$ converges in law to $T_{OU}(x_0, x)$ as $V \rightarrow \infty$.*

Theorem 1.2 ([4]) *Let m be as in Theorem 1.1. Let $M_V(m, \tau) := \max_{0 \leq t \leq \tau} \{X_V(t) | X_V(0) = r(m)\}$ and $M_{OU}(x_0, \tau) := \max_{0 \leq t \leq \tau} \{X_{OU}(t) | X_{OU}(0) = x_0\}$. Then, $M_V(m, \tau)$ converges in law to $M_{OU}(x_0, \tau)$ as $V \rightarrow \infty$.*

2 Uniformization Procedure of Keilson and First Passage Times and Historical Maximum of Markov Chains

Let $N(t)$ be a temporally homogeneous Markov chain in continuous time defined on $\mathcal{N} := \{0, 1, 2, \dots, N\}$, $N \leq \infty$. The process is governed by a set of hazard rates $\{\nu_{mn}\}$ where ν_{mn} is the transition rate from state $m \in \mathcal{N}$ to state $n \in \mathcal{N}$. Then, the infinitesimal generator $\underline{\underline{Q}}$ of $N(t)$ is given by

$$\underline{\underline{Q}} := -\underline{\underline{\nu}}_D + \underline{\underline{\nu}}, \quad (2.1)$$

where

$$\underline{\underline{\nu}} := [\nu_{mn}]; \quad \underline{\underline{\nu}}_D := \text{diag}[\nu_1, \dots, \nu_N]; \quad \nu_m := \sum_{n \in \mathcal{N}} \nu_{mn}. \quad (2.2)$$

The transition probability matrix $\underline{\underline{P}}(t) := [p_{mn}(t)]$, where $p_{mn}(t) := P\{N(t) = n \mid N(0) = m\}$, satisfies the Kolmogorov's matrix differential equation given by

$$\frac{d}{dt} \underline{\underline{P}}(t) = \underline{\underline{Q}} \underline{\underline{P}}(t). \quad (2.3)$$

It then follows that

$$\underline{\underline{P}}(t) = e^{t \underline{\underline{Q}}}. \quad (2.4)$$

The process is said to be *uniformizable* if its hazard rates $\{\nu_{mn}\}$ are bounded in the sense that $\nu_m \leq \nu$ for all $m \in \mathcal{N}$ for some $0 < \nu < \infty$, see Keilson [3]. For a uniformizable chain with a constant ν , let $\underline{\underline{a}}_\nu$ be a matrix defined by

$$\underline{\underline{a}}_\nu := \underline{\underline{I}} - \frac{1}{\nu} \underline{\underline{\nu}}_D + \frac{1}{\nu} \underline{\underline{\nu}}. \quad (2.5)$$

It is clear that the matrix $\underline{\underline{a}}_\nu$ is stochastic, i.e., $\underline{\underline{a}}_\nu \geq \underline{\underline{0}}$, $\underline{\underline{a}}_\nu \underline{\underline{1}} = \underline{\underline{1}}$. From Eqs.(2.1) and (2.5), one has $\underline{\underline{Q}} = -\nu (\underline{\underline{I}} - \underline{\underline{a}}_\nu)$. Substituting this into Eq.(2.4), it then follows that

$$\underline{\underline{P}}(t) = \exp \left\{ -\nu t (\underline{\underline{I}} - \underline{\underline{a}}_\nu) \right\} = \sum_{k=0}^{\infty} e^{-\nu t} \frac{(\nu t)^k}{k!} \underline{\underline{a}}_\nu^k. \quad (2.6)$$

It should be noted that $\underline{\underline{P}}(t)$ can be computed via Eq.(2.6) independently of ν satisfying $\nu \geq \sup_m \nu_m$. Furthermore, since the expression involves only nonnegative numbers, the computational procedure is very stable, enabling one to deal with a fairly large state space,

say, in the order of 10,000. In what follows, we describe computational algorithms for evaluating distributions of first passage times and the historical maximum of the underlying Markov chain based on Eq.(2.6).

Let $G \subset \mathcal{N}$ be a set of “G”ood states and define a set of “B”ad states by $B := \mathcal{N} \setminus G$. Of interest is the first passage time from a good state $m \in G$ to the bad set B defined by

$$T_{m,B} := \inf \{ t \mid N(t) \in B, N(0) = m \} . \quad (2.7)$$

For computing the distributions of such first passage times, we introduce the lossy process $N^*(t)$ obtained from the original process $N(t)$ by making all the states in B absorbing. More specifically, the transition probability matrix $\underline{\underline{P}}^*(t)$ of the lossy process is given by

$$\underline{\underline{P}}^*(t) := \begin{pmatrix} \underline{\underline{P}}_{GG}(t) & \underline{\underline{P}}_{GB}(t) \\ \underline{\underline{Q}} & \underline{\underline{I}} \end{pmatrix} . \quad (2.8)$$

It is clear that the first passage time $T_{m,B}$ is greater than τ if and only if $N(t)$ does not reach B during the period $[0, \tau]$ starting with $N(0) = m \in G$. From the definition of the lossy process, the latter probability can be expressed as

$$\mathbb{P} \{ N(t) \in G \text{ for all } t \in [0, \tau] \mid N(0) = m \in G \} = \mathbb{P} \{ N^*(\tau) \in G \mid N^*(0) = m \in G \} . \quad (2.9)$$

Consequently, the survival function of the first passage time $T_{m,B}$ for $m \in G$ is given by

$$\overline{S}_{m,B}(\tau) := \mathbb{P} \{ T_{m,B} > \tau \} = \mathbb{P} \{ N^*(\tau) \in G \mid N^*(0) = m \in G \} = \underline{\underline{u}}_m^\top \underline{\underline{P}}_{GG}(\tau) \underline{\underline{1}}, \quad (2.10)$$

and the distribution function $S_{m,B}(t)$ by

$$S_{m,B}(t) := 1 - \overline{S}_{m,B}(t). \quad (2.11)$$

Applying Eqs.(2.6) and (2.8), one can see that

$$\underline{\underline{P}}_{GG}(t) = \sum_{k=0}^{\infty} e^{-\nu t} \frac{(\nu t)^k}{k!} \underline{\underline{a}}_{\nu:GG}^k . \quad (2.12)$$

From Eqs.(2.10) and (2.12), it then follows that

$$\overline{S}_{m,B}(t) = \sum_{k=0}^{\infty} e^{-\nu t} \frac{(\nu t)^k}{k!} \underline{\underline{u}}_m^\top \underline{\underline{a}}_{\nu:GG}^k \underline{\underline{1}}. \quad (2.13)$$

Hence, $\overline{S}_{m,B}(t)$ and $S_{m,B}(t)$ can be readily computed via Eq.(2.13) through repeated vector-matrix multiplications.

When the underlying Markov chain $N(t)$ is a birth-death process, all the states are readily ordered and the historical maximum process may be of interest. Let upward and downward transition rates be defined by

$$\nu_{mn} = \begin{cases} \lambda_m & \text{if } n = m + 1, \ m \geq 0 \\ \mu_m & \text{if } n = m - 1, \ m \geq 1 \\ 0 & \text{otherwise} \end{cases} . \quad (2.14)$$

Let $M(m, \tau)$ be the historical maximum of the birth-death process $N(t)$ in the time interval $[0, \tau]$ given that $N(0) = m$, i.e.,

$$M(m, \tau) := \max_{0 \leq t \leq \tau} \{ N(t) \mid N(0) = m \} . \quad (2.15)$$

From the dual relationship between the first passage time and the historical maximum, one sees that

$$F_{m,\tau}(n) := P \{ M(m, \tau) \leq n \} = P \{ T_{m,n+1} > \tau \} = \bar{S}_{m,n+1}(\tau) . \quad (2.16)$$

Consequently, the distribution function of the historical maximum is given by

$$F_{m,\tau}(n) = \begin{cases} 0 & \text{if } n < m \\ \bar{S}_{m,n+1}(\tau) & \text{if } n \geq m \end{cases} , \quad (2.17)$$

where $\bar{S}_{m,n+1}(\tau)$ is the survival function of the first passage time from m to $n + 1$, which is actually the first passage time from m to $B = \{n + 1, n + 2, \dots, N\}$ in Eq.(2.10).

3 O-U Process with One Absorbing Boundary

In this section, by using the convergence results and the uniformization procedure reviewed in the preceding sections, a numerical algorithm is given for evaluating the survival (or equivalently, distribution) function of the first passage times of the modified O-U process with one absorbing boundary. While the uniformization procedure based on Eq.(2.13) involves repeated vector-matrix multiplications, the algorithm developed in this section requires only vector computations since the Ehrenfest process defined in Eq.(1.1) is a birth-death process.

Let $\{N_{2V}(t) : t \geq 0\}$ be the Ehrenfest process on $\mathcal{N}_V = \{0, \dots, 2V\}$ governed by the upward and downward transition rates specified in Eq.(1.1). Since the Ehrenfest process is defined on a finite state space, it is automatically uniformizable. For $m < n$, let $G = \{0, \dots, n - 1\}$ and consider the lossy process $N_{2V}^*(t)$ obtained from $N_{2V}(t)$ by making all the

states in $B = \{n, \dots, 2V\}$ absorbing. Since $N_{2V}(t)$ is a birth-death process and hence is lattice continuous, it is sufficient to consider $N_{2V}^*(t)$ only on $\{0, \dots, n\}$ by making state n absorbing, provided that the process starts with $N_{2V}^*(0) = m \in G$. Since the good set G is on a lower side, we denote the corresponding stochastic matrix on $\{0, \dots, n\}$ by $\underline{a}_{V(L)}^*$. This matrix can be obtained via the uniformization procedure as specified in Eq.(2.5) and is given by

$$\underline{a}_{V(L)}^* := \left(\begin{array}{c|c} \begin{matrix} 0 & \dots & n-1 \end{matrix} & \begin{matrix} n \\ 0 \\ \vdots \\ 0 \\ \frac{\lambda_{n-1}}{V} \end{matrix} \\ \hline \begin{matrix} \underline{a}_{V(L):GG} \end{matrix} & \begin{matrix} 1 \end{matrix} \end{array} \right), \quad (3.1)$$

where

$$\underline{a}_{V(L):GG} = \frac{1}{V} \left(\begin{array}{c|c} \begin{matrix} 0 & 1 & 2 & \dots & n-2 & n-1 \end{matrix} \\ \begin{matrix} 0 & \lambda_0 & 0 & \dots & 0 & 0 \\ \mu_1 & 0 & \lambda_1 & \dots & 0 & 0 \\ 0 & \mu_2 & 0 & \ddots & 0 & 0 \\ \vdots & \vdots & \ddots & \ddots & \ddots & \vdots \\ 0 & 0 & 0 & \ddots & 0 & \lambda_{n-2} \\ 0 & 0 & 0 & \dots & \mu_{n-1} & 0 \end{matrix} \end{array} \right) \begin{matrix} 0 \\ 1 \\ 2 \\ \vdots \\ n-2 \\ n-1 \end{matrix}. \quad (3.2)$$

When G is on an upper side, i.e., $G = \{n+1, \dots, 2V\}$, the corresponding stochastic matrix denoted by $\underline{a}_{V(U)}^*$ is obtained similarly as

$$\underline{a}_{V(U)}^* := \left(\begin{array}{c|c} \begin{matrix} n & n+1 & \dots & 2V \end{matrix} \\ \begin{matrix} 1 \\ \frac{\mu_{n+1}}{V} \\ 0 \\ \vdots \\ 0 \end{matrix} & \begin{matrix} \underline{a}_{V(U):GG} \end{matrix} \end{array} \right), \quad (3.3)$$

where

$$\underline{a}_{V(U):GG} = \frac{1}{V} \left(\begin{array}{c|c} \begin{matrix} n+1 & n+2 & n+3 & \dots & 2V-1 & 2V \end{matrix} \\ \begin{matrix} 0 & \lambda_{n+1} & 0 & \dots & 0 & 0 \\ \mu_{n+2} & 0 & \lambda_{n+2} & \dots & 0 & 0 \\ 0 & \mu_{n+3} & 0 & \ddots & 0 & 0 \\ \vdots & \vdots & \ddots & \ddots & \ddots & \vdots \\ 0 & 0 & 0 & \ddots & 0 & \lambda_{2V-1} \\ 0 & 0 & 0 & \dots & \mu_{2V} & 0 \end{matrix} \end{array} \right) \begin{matrix} n+1 \\ n+2 \\ n+3 \\ \vdots \\ 2V-1 \\ 2V \end{matrix}. \quad (3.4)$$

In either case, one sees from Eq.(2.12) that

$$\begin{cases} \underline{P}_{V(L):GG}^*(t) = \sum_{k=0}^{\infty} e^{-Vt} \frac{(Vt)^k}{k!} (\underline{a}_{V(L):GG})^k \in \mathbb{R}^{|G| \times |G|} \\ \underline{P}_{V(U):GG}^*(t) = \sum_{k=0}^{\infty} e^{-Vt} \frac{(Vt)^k}{k!} (\underline{a}_{V(U):GG})^k \in \mathbb{R}^{|G| \times |G|} \end{cases} \quad (3.5)$$

The survival function $\overline{S}_{x_0,x}(\tau)$ of the first passage time of $X_{OU}(t)$ from x_0 to x is then approximated by the survival function $\overline{S}_{V:m,n}(t)$ of the first passage time of $N_V(t)$ from m to n where $m = \eta_V(x_0) + V$ and $n = \eta_V(x) + V$, which is obtained from Eq.(3.5) as

$$\overline{S}_{V:m,n}(t) = \begin{cases} \sum_{k=0}^{\infty} e^{-Vt} \frac{(Vt)^k}{k!} \underline{u}_m^\top (\underline{a}_{V(L):GG})^k \mathbf{1}, & \text{for } m \in G = \{0, 1, \dots, n-1\} \\ \sum_{k=0}^{\infty} e^{-Vt} \frac{(Vt)^k}{k!} \underline{u}_m^\top (\underline{a}_{V(U):GG})^k \mathbf{1}, & \text{for } m \in G = \{n+1, \dots, 2V\}. \end{cases} \quad (3.6)$$

For the historical maximum $M_V(m, \tau) := \max_{0 \leq t \leq \tau} \{X_V(t) \mid X_V(0) = r(m)\}$, the distribution function $F_{V:m,\tau}(n)$ satisfies the following dual relation as Eq.(2.16):

$$F_{V:m,\tau}(n) = P\{M_V(m, \tau) \leq r(n)\} = P\{T_{V:m,n+1} > \tau\} = \overline{S}_{V:m,n+1}(\tau). \quad (3.7)$$

The distribution function $F_{V:m,\tau}(n)$ of the historical maximum of the O-U process can be computed from Eqs.(2.17) and (3.6).

By exploiting the structure of any birth-death process, the computation for Eq.(3.6) can be simplified. Let \underline{b} be a matrix of the form

$$\underline{b} = \begin{pmatrix} 0 & 1 & 2 & \cdots & n-2 & n-1 \\ 0 & \eta_0 & 0 & \cdots & 0 & 0 \\ \xi_1 & 0 & \eta_1 & \cdots & 0 & 0 \\ 0 & \xi_2 & 0 & \ddots & 0 & 0 \\ \vdots & \vdots & \ddots & \ddots & \ddots & \vdots \\ 0 & 0 & 0 & \ddots & 0 & \eta_{n-2} \\ 0 & 0 & 0 & \cdots & \xi_{n-1} & 0 \end{pmatrix} \begin{matrix} 0 \\ 1 \\ 2 \\ \vdots \\ n-2 \\ n-1 \end{matrix} \in \mathbb{R}^{n \times n}. \quad (3.8)$$

For any n -dimensional real vector $\underline{z} := (z_0, z_1, \dots, z_{n-1})^\top \in \mathbb{R}^n$, let \underline{z}^0 and $\underline{z}^1 \in \mathbb{R}^{n-1}$ be defined by $\underline{z}^0 := (z_0, z_1, \dots, z_{n-2})$ and $\underline{z}^1 := (z_1, z_2, \dots, z_{n-1})$, respectively. We also define an operator \otimes by $\underline{w} \otimes \underline{y} = (w_1 y_1, w_2 y_2, \dots, w_n y_n)$. Then, for $\underline{\eta} := (\eta_0, \eta_1, \dots, \eta_{n-2})$, and $\underline{\xi} := (\xi_1, \xi_2, \dots, \xi_{n-1})$, one has

$$\underline{z}^\top \underline{b} = (0, \underline{z}^0 \otimes \underline{\eta}) + (\underline{z}^1 \otimes \underline{\xi}, 0) \in \mathbb{R}^n. \quad (3.9)$$

We are now in a position to describe an algorithm for computing the survival function $\overline{S}_{V:m,n}(t)$ in Eq.(3.6), where a generic symbol $\underline{a}_{V:GG}$ is employed for $\underline{a}_{V(L):GG}$ and $\underline{a}_{V(U):GG}$.

Algorithm 3.1 (Survival Function of the First Passage Time of the O-U Process from x_0 to x)

Input :

- ▷ V : parameter to describe the range $[x_L, x_U]$ of the O-U process by $2V + 1$ points
- ▷ $n \in \mathcal{N}_V$: the absorbing state with $B = \{n\}$ where $n = \eta_V(x) + V$
- ▷ G : the good set consisting of all the states on either the lower side or the upper side of n
- ▷ $m \in G$: the state from which $N(t)$ starts where $m = \eta_V(x_0) + V$
- ▷ τ : future time as the argument of the survival function
- ▷ $\varepsilon_{\max}, \varepsilon_{\min}$: parameters for stopping criteria for the series expansion of Eq.(3.6)

- 1) Set $s_{m,n} \leftarrow 0$, $k \leftarrow 0$ and $\underline{x} \leftarrow \underline{u}_m$.
- 2) Set $K = \max \left\{ k : e^{-V\tau} \frac{(V\tau)^k}{k!} < \varepsilon_{\max} \right\}$ and $k_0 = \min \left\{ k : e^{-V\tau} \frac{(V\tau)^k}{k!} > \varepsilon_{\min} \right\}$
- 3) LOOP1: $\underline{x}^\top \leftarrow \underline{x}^\top \underline{a}_{V:GG}$.
- 4) If $k < k_0$, set $k \leftarrow k + 1$ and go to LOOP1.
- 5) LOOP2: $s_{m,n} \leftarrow s_{m,n} + e^{-V\tau} \frac{(V\tau)^k}{k!} \underline{x}^\top \underline{1}$.
- 6) If $k < K$, set $\underline{x}^\top \leftarrow \underline{x}^\top \underline{a}_{V:GG}$, $k \leftarrow k + 1$, and go to LOOP2.
- 7) Stop.

Remark 3.2: For computational stability in evaluating the sequence $\left\{ e^{-V\tau} \frac{(V\tau)^k}{k!} \right\}_{k=1,2,\dots}$, we used the following recurrence formula of $b(V, k, \tau) := \ln e^{-V\tau} \frac{(V\tau)^k}{k!}$:

$$b(V, k, \tau) = b(V, k - 1, \tau) + \ln \frac{V\tau}{k}.$$

Figure 3.1(a) shows the survival function of the first passage time $T_V(m, n)$ of $X_V(t)$ from $m = \eta_V(0) + V = V$ to $n = \eta_V(1) + V$ for $V = 200$. A sequence of such survival functions converges in law to that of the first passage time $T_{OU}(0, 1)$ of $X_{OU}(t)$ from 0 to 1 as $V \rightarrow \infty$. In Figure 3.1(b), this convergence is demonstrated by plotting $\left\| \bar{S}_{V:m,n} - \bar{S}_{800:m,n} \right\|_\infty = \sup \left\{ \left| \bar{S}_{V:m,n}(\tau) - \bar{S}_{800:m,n}(\tau) \right| : \tau \in [0, 10] \right\}$ from $V = 200$ to $V = 800$ with step size of 50,

and the supremum is taken with step size of $\Delta t = 0.1$. One observes that almost 4-digit accuracy is attained with speed at $V = 800$. The convergence is not monotone because the relative location of $x = 1$ within a discretized interval of the width $\Delta x = \sqrt{\frac{2}{V}}$ does not change monotonically as V increases.

[Figure 3.1]

To examine the convergence behavior from a different angle, the median value of the first passage time is computed as a function of V . Formally, this is defined as $\tau^*(x_0, x) := \overline{S}_{V:m,n}^{-1}(0.5)$, where $m = \eta_V(x_0) + V$ and $n = \eta_V(x) + V$. We call $\tau^*(x_0, x)$ the median time. Table 3.1 shows the computed median time $\tau^*(x_0, x)$ of the approximating process $X_V(t)$ from x_0 to a boundary point x for $x_0 = 0, 0.5$ and $x = 1, 2$. Only the results for V satisfying $x_0 = \sqrt{\frac{2}{V}}\eta_V(x_0)$ are shown. From this table, we see that the median time can be computed with 3-digit accuracy.

[Table 3.1]

We next turn our attention to the historical maximum of $X_V(t)$, which approximates that of $X_{OU}(t)$. Figure 3.2(a) displays the convergence of the distribution functions of the historical maximum of the process with $x_0 = 0$ by varying V from 200 to 800. The enlarged view is provided in Figure 3.2(b). One sees that the speed of convergence is slower for the historical maximum than the first passage time.

[Figure 3.2]

Table 3.2 shows the median point $x^*(x_0, \tau) := F_{x_0, \tau}^{-1}(0.5)$ of the historical maximum distribution until time τ when starting from a given point x_0 for $x_0 = 0, 0.5$ and $\tau = 1, 10$. From this table, we see that the median point can be computed with 4-digit accuracy.

[Table 3.2]

4 O-U Process with Two Absorbing Boundaries

In this section, modified O-U processes with two absorbing boundaries are considered. Let x_1 and x_2 be the down and the upper boundaries respectively and define $\overline{S}_{x_0, (x_1, x_2)}(t) = P\{T_{x_0, (x_1, x_2)} > t\}$ where $T_{x_0, (x_1, x_2)}$ is the first passage time of the modified O-U process from $x_0 \in (x_1, x_2)$ to either x_1 or x_2 . The corresponding approximation $\overline{S}_{V:m, (n_1, n_2)}(t)$ with

$m = \eta_V(x_0) + V$, $n_1 = \eta_V(x_1) + V$ and $n_2 = \eta_V(x_2) + V$ can be evaluated via the uniformization procedure as for the case of one absorbing boundary. The stochastic matrix \underline{a}_V^* of interest becomes

$$\underline{a}_V^* := \left(\begin{array}{c|ccc|c} n_1 & n_1+1 & \dots & n_2-1 & n_2 \\ \hline 1 & \underline{0}^\top & & & 0 \\ \hline \frac{\mu_{n_1+1}}{V} & & & & 0 \\ 0 & & & & 0 \\ \vdots & & \underline{a}_{V:GG} & & \vdots \\ 0 & & & & 0 \\ 0 & & & & \frac{\lambda_{n_2-1}}{V} \\ \hline 0 & \underline{0}^\top & & & 1 \end{array} \right), \quad (4.1)$$

where

$$\underline{a}_{V:GG} = \frac{1}{V} \left(\begin{array}{cccccc} n_1+1 & n_1+2 & n_1+3 & \dots & n_2-2 & n_2-1 \\ 0 & \lambda_{n_1+1} & 0 & \dots & 0 & 0 \\ \mu_{n_1+2} & 0 & \lambda_{n_1+2} & \dots & 0 & 0 \\ 0 & \mu_{n_1+3} & 0 & \ddots & 0 & 0 \\ \vdots & \vdots & \ddots & \ddots & \ddots & \vdots \\ 0 & 0 & 0 & \ddots & 0 & \lambda_{n_2-2} \\ 0 & 0 & 0 & \dots & \mu_{n_2-1} & 0 \end{array} \right) \begin{array}{l} n_1+1 \\ n_1+2 \\ n_1+3 \\ \vdots \\ n_2-2 \\ n_2-1 \end{array}. \quad (4.2)$$

From (2.13), it then follows that

$$\overline{S}_{V:m,(n_1,n_2)}(\tau) = \sum_{k=0}^{\infty} e^{-V\tau} \frac{(V\tau)^k}{k!} \underline{a}_m^\top (\underline{a}_{V:GG})^k \underline{1}, \text{ for } m \in G = \{n_1+1, \dots, n_2-1\}. \quad (4.3)$$

For the historical maximum $M_V^+(m, \tau) := \max_{0 \leq t \leq \tau} \{|X_V(t)| \mid X_V(0) = r(m)\}$, the distribution function $F_{V:m,\tau}^+(n_1, n_2)$ satisfies the following dual relation as before:

$$\begin{aligned} F_{V:m,\tau}^+(n_1, n_2) &= \mathbb{P} \{ r(n_1) \leq M_V(m, \tau) \leq r(n_2) \} \\ &= \mathbb{P} \{ T_{m,(n_1-1,n_2+1)} > \tau \} \\ &= \overline{S}_{V:m,(n_1-1,n_2+1)}(\tau), \end{aligned} \quad (4.4)$$

where $n_2 = 2V - n_1 \geq V$. Consequently, corresponding to Eq.(2.16), it follows that

$$F_{V:m,\tau}^+(n_1, n_2) = \begin{cases} \overline{S}_{V:m,(n_1,n_2)}(\tau) & \text{for } m \in \{n_1 + 1, \dots, n_2 - 1\} \\ 0 & \text{for } m \in \{0, \dots, n_1 - 1\} \text{ or } m \in \{n_2 + 1, \dots, 2V\} \\ 1 & \text{for } m = n_1 \text{ or } n_2 \end{cases}. \quad (4.5)$$

Both $\overline{S}_{V:m,(n_1,n_2)}(\tau)$ and $F_{V:m,\tau}^+(n_1, n_2)$ can be readily computed by an algorithm similar to Algorithm 3.1. Because of this similarity, the description of the algorithm is omitted here.

It should be noted that the first passage time of the absolute value process $|X_{OU}(t)|$ is a special case with $x_1 = -x$ and $x_2 = x$ for $x > 0$. Let $T_{OU}^+(x_0, x)$ be the first passage time of $|X_{OU}(t)|$ defined by $T_{OU}^+(x_0, x) := \inf \{ t : |X_{OU}(t)| = x \mid X_{OU}(0) = x_0 \}$ for $x \geq 0$. The corresponding survival function is denoted by $\bar{S}_{OU:x_0,x}^+(\tau) := P \{ T_{OU}^+(x_0, x) > \tau \}$. Figure 4.1(a) shows $\bar{S}_{OU:x_0,x}^+(\tau)$ with $V = 200$ for $x_0 = 0$ and $x = 1$, and Figure 4.1(b) demonstrates the speed of convergence of such survival functions as V varies from 200 to 800 with step size of 50. Almost 4-digit accuracy is attained with speed at $V = 800$. As for Figure 3.1(b), the convergence is not monotone.

[Figure 4.1]

Corresponding to Table 3.1, the median times of $|X_V(t)|$ are exhibited in Table 4.1 for $x_0 = 0$, $x_1 = -1, -2$ and $x_2 = 1, 2$. One observes that the median time can be computed with 3-digit accuracy.

[Table 4.1]

Figure 4.2(a) shows the distribution functions of the historical maximum of the absolute value process for V from 200 to 800 with step size of 50. These graphs are enlarged in Figure 4.2(b) so as to see the convergence speed better. Table 4.2 shows the median value of the historical maximum of the absolute value process with 3-digit accuracy.

[Figure 4.2]

[Table 4.2]

5 O-U Process with Two Replacement and Reflection Boundaries

In contrast with absorbing boundaries discussed in the previous two sections, a replacement boundary moves the process to a state in G according to a certain probability law as soon as the process reaches B . The purpose of this section is to establish a numerical algorithm to capture the dynamic behavior of modified O-U processes with such replacement boundaries. The relationship between a modified O-U process with one replacement boundary and that with two replacement boundaries is similar to the relationship for absorbing boundaries. Because of this, only the cases of two replacement boundaries are discussed here.

We say that $\{X_{OU}^{RP}(t) : t \geq 0\}$ has two replacement boundaries at x_L and x_U with replacement probability density functions $r_L(x)$ and $r_U(x)$ respectively if an instantaneous replacement to state $x \in (x_L, x_U)$ occurs according to $r_L(x)$ or $r_U(x)$ as soon as the process reaches x_L or x_U , respectively. Figure 5.1(a) illustrates the movement of a modified O-U process with two replacement boundaries. The movement of the approximating process $\{X_V^{RP}(t) : t \geq 0\}$ is depicted in Figure 5.1(b), where the replacement probability vectors \underline{r}_L and \underline{r}_U are employed instead of $r_L(x)$ and $r_U(x)$.

[Figure 5.1]

It should be noted that replacements for $X_V^{RP}(t)$ occur as soon as the process reaches either $r(n_1)$ or $r(n_2)$ starting from $r(m)$ where $m = \eta_V(x_0) + V$, $n_1 := \eta_V(x_L) + V$, and $n_2 := \eta_V(x_U) + V$. As in Eq.(1.5), the relationship between $X_V^{RP}(t)$ and the associated Ehrenfest process $N_{2V}^{RP}(t)$ is given by

$$X_V^{RP}(t) = \sqrt{\frac{2}{V}} N_{2V}^{RP}(t) - \sqrt{2V}. \quad (5.1)$$

It can be readily seen that $N_{2V}^{RP}(t)$ has the transition probability matrix $\underline{\underline{P}}^{RP}(t)$ given via the uniformization procedure as

$$\underline{\underline{P}}^{RP}(t) = \sum_{k=0}^{\infty} e^{-Vt} \frac{(Vt)^k}{k!} \underline{\underline{a}}_V^{RP k}, \quad (5.2)$$

where

$$\underline{\underline{a}}_V^{RP} = \left(\begin{array}{c|c|c} 0 & \underline{r}_L^\top & 0 \\ \hline \frac{\mu_{n_1+1}}{V} & & 0 \\ 0 & \underline{\underline{a}}_{V(n_1+1:n_2-1)} & 0 \\ 0 & & \frac{\lambda_{n_2-1}}{V} \\ \hline 0 & \underline{r}_U^\top & 0 \end{array} \right) \quad (5.3)$$

and

$$\underline{\underline{a}}_{V(n_1+1:n_2-1)} = \frac{1}{V} \begin{pmatrix} n_1+1 & n_1+2 & n_1+3 & \cdots & n_2-2 & n_2-1 \\ 0 & \lambda_{n_1+1} & 0 & \cdots & 0 & 0 \\ \mu_{n_1+2} & 0 & \lambda_{n_1+2} & \cdots & 0 & 0 \\ 0 & \mu_{n_1+3} & 0 & \ddots & 0 & 0 \\ \vdots & \vdots & \ddots & \ddots & \ddots & \vdots \\ 0 & 0 & 0 & \ddots & 0 & \lambda_{n_2-2} \\ 0 & 0 & 0 & \cdots & \mu_{n_2-1} & 0 \end{pmatrix} \begin{matrix} n_1+1 \\ n_1+2 \\ n_1+3 \\ \vdots \\ n_2-2 \\ n_2-1 \end{matrix}. \quad (5.4)$$

Clearly, $\underline{a}_V^{\text{RP}}$ is ergodic and so is $N_{2V}^{\text{RP}}(t)$ and $X_V^{\text{RP}}(t)$. Hence, of interest is to compute the time dependent tail state probability defined as

$$\overline{G}_V^{\text{RP}}(t, x) := \text{P} \left\{ X_V^{\text{RP}}(t) > x = r(n) \right\} = \text{P} \left\{ N_{2V}^{\text{RP}}(t) > n \right\} = \sum_{k=n+1}^{n_2} p_{mk}^{\text{RP}}(t), \quad (5.5)$$

where $\underline{p}_m^{\text{RP}}(t) := (p_{mn_1}^{\text{RP}}(t), \dots, p_{mn_2}^{\text{RP}}(t))^{\top}$ is computed from Eq.(5.2) by $\underline{p}_m^{\text{RP}}(t)^{\top} = \underline{u}_m^{\top} \underline{P}^{\text{RP}}(t)$. As $V \rightarrow \infty$, $\overline{G}_V^{\text{RP}}(t, x)$ converges to $\overline{G}_{\text{OU}}^{\text{RP}}(t, x) := \text{P} \left\{ X_{\text{OU}}^{\text{RP}}(t) > x = r(n) \right\}$.

Figure 5.2 shows $\overline{G}_V^{\text{RP}}(t, x)$ with $V = 800$, $x_L = -2$, $x_U = 2$, and $t = 0.1, 0.2, \dots, 0.6$, as well as the ergodic distribution

$$\overline{G}_V^{\text{RP}}(\infty, x) = \sum_{k=n+1}^{n_2} e_k^{\text{RP}}, \quad (5.6)$$

where the ergodic vector $\underline{e}^{\text{RP}} := (e_{n_1}^{\text{RP}}, \dots, e_{n_2}^{\text{RP}})^{\top}$ is obtained from Eq.(5.3) by solving $\underline{e}^{\text{RP}\top} = \underline{e}^{\text{RP}\top} \underline{a}_V^{\text{RP}}$ with $\underline{e}^{\text{RP}\top} \underline{1} = 1$. The two replacement probability vectors are taken to be a binomial distribution $r_{Lk} = r_{Uk} = \binom{n}{k} 0.5^k 0.5^{n-k}$, $k = 0, 1, \dots, n = n_2 - n_1 - 1$. One can see that $\overline{G}_V^{\text{RP}}(t, x)$ converges to the ergodic distribution $\overline{G}_V^{\text{RP}}(\infty, x)$ as t increases.

[Figure 5.2]

A modified O-U process with two reflection boundaries at x_L and x_U , denoted by $\{X_{\text{OU}}^{\text{RF}}(t) : t \geq 0\}$, is a special case of $\{X_{\text{OU}}^{\text{RP}}(t) : t \geq 0\}$ with two replacement boundaries at x_L and x_U . More specifically, the approximating process $\{X_V^{\text{RF}}(t) : t \geq 0\}$ has the transition probability matrix $\underline{P}^{\text{RF}}(t)$, which is obtained as

$$\underline{P}^{\text{RF}}(t) = \sum_{k=0}^{\infty} e^{-Vt} \frac{(Vt)^k}{k!} \underline{a}_V^{\text{RF}k}, \quad (5.7)$$

where

$$\underline{a}_V^{\text{RF}} = \left(\begin{array}{c|c|c} 0 & \underline{r}_L^{\top} & 0 \\ \hline \frac{\mu_{n_1+1}}{V} & & 0 \\ 0 & \underline{a}_{V(n_1+1:n_2-1)} & 0 \\ \hline 0 & & \frac{\lambda_{n_2-1}}{V} \\ 0 & \underline{r}_U^{\top} & 0 \end{array} \right) \quad (5.8)$$

with $\underline{r}_L = (1, 0, \dots, 0)^{\top}$, $\underline{r}_U = (0, \dots, 0, 1)^{\top}$, and $\underline{a}_{V(n_1+1:n_2-1)}$ given by Eq.(5.4). Figure 5.3(a) illustrates the movement of $X_{\text{OU}}^{\text{RF}}(t)$ and the movement of the approximating process $X_V^{\text{RF}}(t)$ is depicted in Figure 5.3(b).

[Figure 5.3]

Similarly to Eqs.(5.5) and (5.6), one has

$$\overline{G}_V^{\text{RF}}(t, x) := \mathbb{P} \left\{ X_V^{\text{RF}}(t) > x = r(n) \right\} = \mathbb{P} \left\{ N_{2V}^{\text{RF}}(t) > n \right\} = \sum_{k=n+1}^{n_2} p_{mk}^{\text{RF}}(t), \quad (5.9)$$

and

$$\overline{G}_V^{\text{RF}}(\infty, x) = \sum_{k=n+1}^{n_2} e_k^{\text{RF}}, \quad (5.10)$$

where $\underline{p}_m^{\text{RF}}(t) := (p_{mn_1}^{\text{RF}}(t), \dots, p_{mn_2}^{\text{RF}}(t))^{\top}$ and $\underline{e}^{\text{RF}} := (e_{n_1}^{\text{RF}}, \dots, e_{n_2}^{\text{RF}})^{\top}$ are computed from $\underline{p}_m^{\text{RF}}(t)^{\top} = \underline{u}_m^{\top} \underline{P}^{\text{RF}}(t)$ and $\underline{e}^{\text{RF}\top} = \underline{e}^{\text{RF}\top} \underline{a}_V^{\text{RF}}$ with $\underline{e}^{\text{RF}\top} \underline{1} = 1$, respectively. As before, $\overline{G}_V^{\text{RF}}(t, x)$ converges to $\overline{G}_{\text{OU}}^{\text{RF}}(t, x) := \mathbb{P} \left\{ X_{\text{OU}}^{\text{RF}}(t) > x = r(n) \right\}$ as $V \rightarrow \infty$.

Figure 5.4 shows $\overline{G}_V^{\text{RF}}(t, x)$ and $\overline{G}_V^{\text{RF}}(\infty, x)$ with $V = 800$, $x_L = -2$, $x_U = 2$, and $t = 0.1, 0.2, \dots, 1.0$. One can see that $\overline{G}_V^{\text{RF}}(t, x)$ converges to the ergodic distribution $\overline{G}_V^{\text{RF}}(\infty, x)$ as t increases.

[Figure 5.4]

6 Evaluation of Prices of Up-and-Out Call Options

Barrier options are path-dependent options with payoff dependent on the realized path of the underlying asset value and its prespecified level(s). Normally, an action promised in the contract is taken if the asset value becomes too high or too low, see e.g. [6]. In this section, we consider an up-and-out call option maturing at time τ_M with strike price K_S written on a discount bond of maturity at time T . As discussed in Section 0, with $\widehat{X}_{\text{OU}}(0) = \hat{x}_0$, its price $\pi_{\text{KO}}(\tau_M | \hat{x}_0, T)$ is given by (0.6). Our purpose here is to develop computational procedures for evaluating this price based on the results of the previous sections.

From (0.4) and the proposed Ehrenfest approximation, one sees that

$$\widehat{X}_{\text{OU}}(t) \approx \widetilde{X}_V(t) + \theta(t), \quad (6.1)$$

where

$$\begin{cases} \widetilde{X}_V(t) &= \frac{\sigma}{\sqrt{\alpha V}} \widetilde{N}_{2V}(t) - \sigma \sqrt{\frac{V}{\alpha}}, \\ \theta(t) &= \frac{\phi}{\alpha} (1 - e^{-\alpha t}) + \widehat{X}_{\text{OU}}(0) e^{-\alpha t} \end{cases} \quad (6.2)$$

with $\widetilde{N}_{2V}(t) := N_{2V}(\alpha t)$. For $T = K \Delta t$ and $0 \leq k \leq K$, let $D(k, m | K)$ be the discount bond price at time $\tau = k \Delta t$ at a state corresponding to state $m \in \mathcal{N}_V$ of the underlying Ehrenfest

process. Starting with $D(K, m|K) = 1$ for all $m \in \mathcal{N}_V$, these values can be computed via the following backward recursive formula:

$$D(k, m|K) = e^{-r(k, m)\Delta t} \sum_{n \in \mathcal{N}_V} \tilde{p}_{2V:mn}(\Delta t) D(k+1, n|K), \quad (6.3)$$

where $\tilde{\underline{P}}_{2V}(\Delta t) = [\tilde{p}_{2V:mn}(\Delta t)]$ is the transition probability matrix of $\{\tilde{N}_{2V}(t) : t \geq 0\}$ with time duration of Δt , and

$$r(k, m) = \tilde{x}_V(m) + \theta(k\Delta t) \quad (6.4)$$

with $\tilde{X}_{OU}(k\Delta t) = \tilde{x}_V(m)$.

The barrier condition $\widehat{X}_{OU}(t) \leq r_B$ can be written as

$$\tilde{X}_V(t) \leq r_B - \theta(t), \quad 0 \leq t \leq \tau_M. \quad (6.5)$$

By the state conversion between $\{\tilde{X}_V(t) : t \geq 0\}$ and $\{\tilde{N}_{2V}(t) : t \geq 0\}$ via (6.2), the condition (6.5) can be rewritten as

$$\tilde{N}_{2V}(t) \leq n_B(t); \quad n_B(t) = \tilde{\eta}_V(r_B - \theta(t)) + V, \quad 0 \leq t \leq \tau_M, \quad (6.6)$$

where $\tilde{\eta}_V(x) = \left\lceil \frac{\sqrt{\alpha V}}{\sigma} x \right\rceil$. For notational convenience, we denote the set of states satisfying (6.6) by

$$G(t) := \{m : 0 \leq m \leq n_B(t)\}, \quad 0 \leq t \leq \tau_M. \quad (6.7)$$

In order to evaluate the joint probability of $\tilde{N}_{2V}(t)$ at state $m \in G(t)$ and $\tilde{N}_{2V}(t') \in G(t')$ for all $t' \in [0, t]$, we adopt the one absorbing boundary approach of Section 3 with discretized time axis in the following manner. Given $G(k\Delta t)$, one can construct a lossy process by making the state $n_B(t) + 1$ absorbing. Using (3.1) and (2.6), the transition probability matrix $\underline{\underline{P}}^*(\Delta t)$ of this lossy process with time duration of Δt can be obtained. The desired joint probability at time $t = k\Delta t$, starting at a state $\tilde{N}_{2V}(0) = n_0 \in G(0)$, can then be given by

$$\prod_{j=1}^k \underline{\underline{P}}_{G((j-1)\Delta t)G(j\Delta t)}^*(\Delta t). \quad (6.8)$$

It should be noted that the matrix $\underline{P}^*(\Delta t)$ has to be computed for each $t = k\Delta t$ because of the moving boundary $n_B(t)$, which can be dealt with by connecting submatrices of variable size specified by $G(j\Delta t)$.

For the option under consideration with maturity at $\tau_M = M\Delta t$, let $\pi_{KO}(k, m|M)$ be the option price at time $\tau = k\Delta t$ at state $m \in G(\tau)$. One then sees from (0.6) that the desired price $\pi_{KO}(\tau_M|\hat{x}_0, T)$ can be expressed as

$$\pi_{KO}(\tau_M|\hat{x}_0, T) \approx \pi_{KO}(0, n_0|M), \quad (6.9)$$

where $\widetilde{N}_{2V}(0) = n_0$. The payoff function $h_c(D)$ at time $\tau_M = M\Delta t$ and state $m \in G(\tau_M)$ is given by

$$h_c(D(M, m|K)) = [D(M, m|K) - K_S]^+, \quad (6.10)$$

with K_S as in (0.8). Then the price of the up-and-out call option at node (k, m) with $m \in G(k\Delta t)$ can be evaluated by the following backward scheme:

$$\pi_{KO}(k, m|M) = e^{-r(k, m)\Delta t} \sum_{n \in G((k+1)\Delta t)} p_{2V:mn}^*(\Delta t) \pi_{KO}(k+1, n|M), \quad (6.11)$$

starting with $\pi_{KO}(M, m|M) = h_c(D(M, m|K))$, where $r(k, m)$ is as given in (6.4). The desired price $\pi_{KO}(\tau_M|\hat{x}_0, T)$ can then be obtained from (6.9) by repeating (6.11) until $k = 0$ and $m = n_0$.

The above discussion is now summarized below. It should be noted that the time axis should be discretized satisfying $T = K\Delta t$ and $\tau_M = M\Delta t$.

Algorithm 6.1 (Up-And-Out Call Option Pricing)

Input :

- ▷ V : size of the state space of $\{\widetilde{N}_{2V}(t) : t \geq 0\}$
- ▷ T : maturity time of the discount bond
- ▷ τ_M : maturity time of the option
- ▷ Δt : discretized time interval satisfying $T = K\Delta t$ and $\tau_M = M\Delta t$ for some positive integers K and M

▷ \hat{x}_0 : initial interest rate

▷ r_B : prespecified upper limit of the interest rate

▷ r_S : prespecified rate which determines the strike price of the option

▷ α : reversion factor

▷ σ : volatility factor

▷ ϕ : mean reversion level

- 1) Determine $G(M\Delta t)$ and compute $\pi_{\text{KO}}(M, m|M) = [D(M, m|K) - K_S]^+$ for all $m \in G(M\Delta t)$, where $K_S = e^{-r_S(T-\tau_M)}$.
- 2) Set $k = M - 1$.
- 3) LOOP: Evaluate $\underline{P}^*(\Delta t) = [p_{2V:mn}^*(\Delta t)]$ of size $(n_B(k\Delta t) + 2) \times (n_B(k\Delta t) + 2)$.
- 4) Find $G(k\Delta t)$ and compute

$$\pi_{\text{KO}}(k, m|M) = e^{-r(k,m)\Delta t} \sum_{n \in G((k+1)\Delta t)} p_{2V:mn}^*(\Delta t) \pi_{\text{KO}}(k+1, n|M)$$

for all $m \in G(k\Delta t)$.

- 5) If $k = 0$, stop. Otherwise set $k = k - 1$ and goto LOOP.

For comparison purpose, the Hull-White trinomial tree approach is modified to deal with the same up-and-out call option discussed above. We note that, for the Hull-White trinomial tree approach, the maximum positive integer m_k corresponding to the highest node at time $k\Delta t$ should satisfy

$$\left\lceil \frac{3 - \sqrt{6}}{3\alpha\Delta t} \right\rceil \leq m_k \leq \left\lfloor \frac{\sqrt{6}}{3\alpha\Delta t} \right\rfloor, \quad (6.12)$$

where $\lceil a \rceil$ denotes the minimum integer which is greater than or equal to a , and $\lfloor a \rfloor$ the maximum integer which is smaller than or equal to a . Let $m_l = \left\lceil \frac{3 - \sqrt{6}}{3\alpha\Delta t} \right\rceil$. For certain low values of r_B 's, when Δt is fixed, it is possible that $r_B - \theta(k\Delta t) < m_l \Delta \tilde{x}$ where $\Delta \tilde{x} = \sigma \sqrt{3\Delta t}$ (see Hull [2]). If this happened, the trinomial tree can not be constructed. In order to see this point, we consider the following examples with $\phi = 0.05$, $\alpha = 0.2$, $\sigma = 0.01$, $\hat{x}_0 = 0.05$,

$T = 5$, $\tau_M = 4$, $r_S = 0.2$ and $r_B = 0.25$. In Tables 6.1(a) and (b) and Figures 6.1(a) and (b), “Ehrenfest” or “Ehrenfest approach” indicates that the results are calculated by the Ehrenfest approach, and “HW tree” or “HW trinomial tree” by the Hull-White trinomial tree approach. For $50 \leq M \leq 120$, the relative errors of the price values computed by the two approaches are bounded by 0.2%. However, it is found that the trinomial tree approach cannot be employed for $M > 122$. Indeed, when choosing $M = 123$, $r_B - \theta(M\Delta t) = 0.0905 < m_l\Delta\tilde{x} = 0.0906$ and the Hull-White trinomial tree approach collapses. The Ehrenfest approach does not suffer from this limitation, as demonstrated in Table (6.1)(b) and Figure 6.1(b) where the price values between $M = 120$ and 250 with the same parameters are exhibited.

[Table 6.1(a)]

[Table 6.1(b)]

[Figure 6.1(a)] [Figure 6.1(b)]

Acknowledgement This research is partly supported by Mizuho-Daiichi Financial Technologies, co. The first author is supported by MEXT Grant-in-Aid for Young Scientists (B) 17710125. The third author is supported by MEXT Grant-in-Aid for Scientific Research (C) 17510114. Also, the authors appreciate the useful comments by Professor Steven Finch.

References

- [1] FELLER, W., *An Introduction to Probability Theory and Its Applications, Vol.2*, 2nd ed. Wiley, New York, 1966.
- [2] Hull, J., *Options, Futures and Other Derivatives*, 4th edn. Prentice-Hall International, Inc. 2000.
- [3] KEILSON, J., *Markov Chain Models: Rarity and Exponentiality*, (Applied Mathematical Science Series, 28), Springer, New York, 1979.
- [4] SUMITA, U., GOTOH, J., & JIN, H., Numerical Exploration of Dynamic Behavior of Ornstein-Uhlenbeck Processes via Ehrenfest Process Approximation. *Journal of the Operations Research Society of Japan*, to appear.
- [5] VASICEK, O., An Equilibrium Characterization of the Term Structure. *Journal of Financial Economics* 5, pp.177–188, 1977.
- [6] Wilmott, P. *Derivatives: the Theory and Practice of Financial Engineering*, John Wiley and Sons Ltd, England, 1998.

Table 1.1: State Conversions

Process	State Conversion		State Space
	$x \in \mathbb{R} \rightarrow m \in \mathcal{N}$	$m \in \mathcal{N} \rightarrow x \in \mathbb{R}$	
$N_V(t)$	$\eta_V(x) + V$	m	$\mathcal{N} = \{0, 1, \dots, 2V\}$
$X_V(t)$	$\sqrt{\frac{2}{V}}\eta_V(x)$	$r(m)$	$\{-\sqrt{2V}, \dots, \sqrt{2V}\}$

Table 3.1: Median Time of First Passage Time of X_{OU} ($\Delta t = 0.1$)

V	$\Delta x = \sqrt{\frac{2}{V}}$	$\tau^*(0, 1)$	$\tau^*(0, 2)$	$\tau^*(0.5, 1)$	$\tau^*(0.5, 2)$
200	0.1	1.18772	7.24733	0.38715	6.38354
800	0.05	1.18912	7.25101	0.38748	6.38650
3,200	0.025	1.18947	7.25192	0.38757	6.38723
5,000	0.02	1.18951	7.25203	0.37882	6.38732
20,000	0.01	1.18956	7.25218	0.37889	6.38737

Table 3.2: Median Point of Historical Maximum $M(x_0, \tau)$ of $X_{OU}(t)$

V	$\Delta x = \sqrt{\frac{2}{V}}$	$x^*(0, 1)$	$x^*(0, 10)$	$x^*(0.5, 1)$	$x^*(0.5, 10)$
200	0.1	0.92412	2.17776	1.24186	2.22067
800	0.05	0.92337	2.17765	1.24095	2.22057
3,200	0.025	0.92315	2.17759	1.24081	2.22052
5,000	0.02	0.92313	2.17758	1.24076	2.22052
20,000	0.01	0.92311	2.17758	1.24076	2.22052

Table 4.1: Median Time of First Passage Time of $|X_V(t)|$

V	$\Delta x = \sqrt{\frac{2}{V}}$	$\tau_{0,(-1,1)}^*$	$\tau_{0,(-2,2)}^*$	$\tau_{0.5,(-1,1)}^*$	$\tau_{0.5,(-2,2)}^*$
200	0.1	0.44659	3.24198	0.30079	3.11018
800	0.05	0.44721	3.24366	0.30142	3.11172
3,200	0.025	0.44736	3.24408	0.30158	3.11211
5,000	0.02	0.44738	3.24413	0.30160	3.11215
20,000	0.01	0.44740	3.24419	0.30162	3.11218

Table 4.2: Median Point of Historical Maximum of $|X_V(t)|$

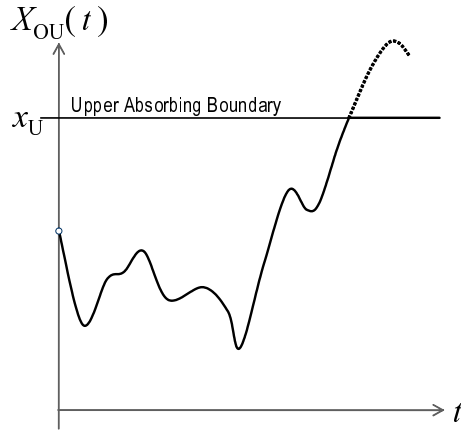
V	$\Delta x = \sqrt{\frac{2}{V}}$	$x_{0,1}^*$	$x_{0,10}^*$	$x_{0.5,1}^*$	$x_{0.5,10}^*$
200	0.1	1.38328	2.54814	1.44852	2.55399
800	0.05	1.38239	2.54823	1.44707	2.55409
3,200	0.025	1.38207	2.54837	1.44691	2.55422
5,000	0.02	1.38201	2.54840	1.44690	2.55424
20,000	0.01	1.38201	2.54840	1.44690	2.55424

Table 6.1: Up-and-Out Option Prices via Different Time Steps
(a) $M = 50$ to 120

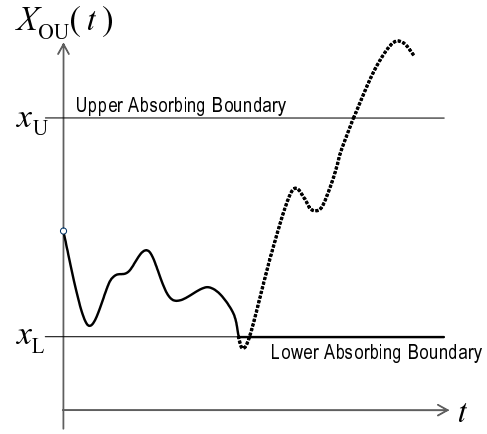
M	50	60	70	80	90	100	110	120
Ehrenfest	0.017404	0.017341	0.017287	0.017252	0.017219	0.017196	0.017173	0.017156
HW Tree	0.017373	0.017308	0.017254	0.017218	0.017187	0.017165	0.017145	0.017129
Relative Errors	0.1772%	0.1888%	0.1919%	0.1971%	0.1866%	0.1815%	0.1659%	0.1554%

(b) $M = 120$ to 250

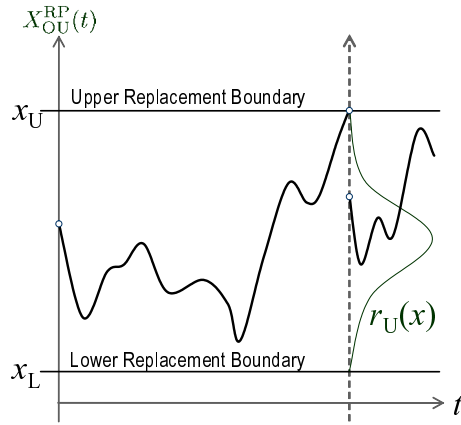
M	130	150	170	190	210	230	240	250
Ehrenfest	0.017138	0.017110	0.017087	0.017067	0.017050	0.017034	0.017027	0.017020



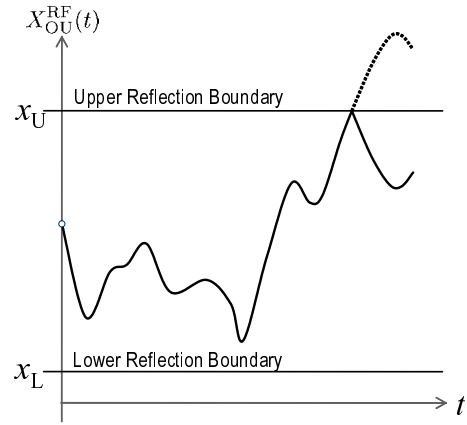
(a) Single Absorbing Boundary



(b) Double Absorbing Boundaries

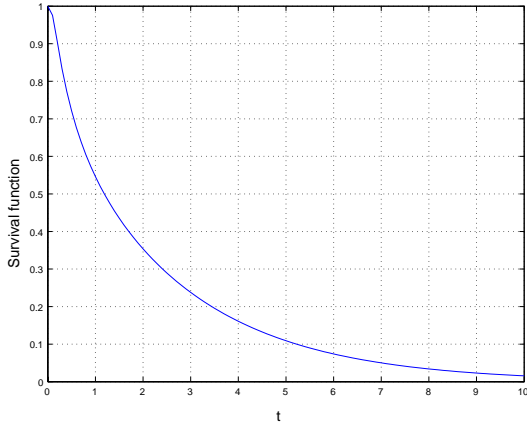


(c) Double Replacement Boundaries

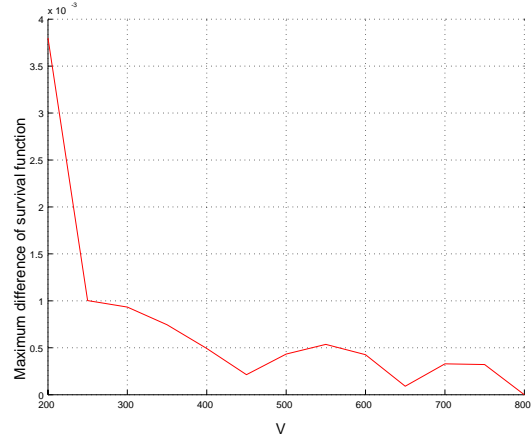


(d) Double Reflection Boundaries

Figure 0.1: Modified O-U Processes with Various Boundaries

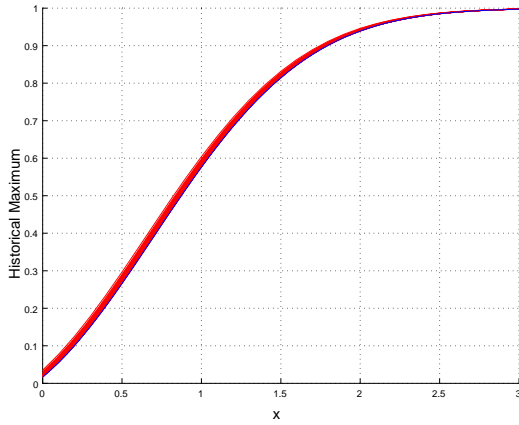


(a) Survival Function $S_{V:m,n}(t)$ with $V = 200$

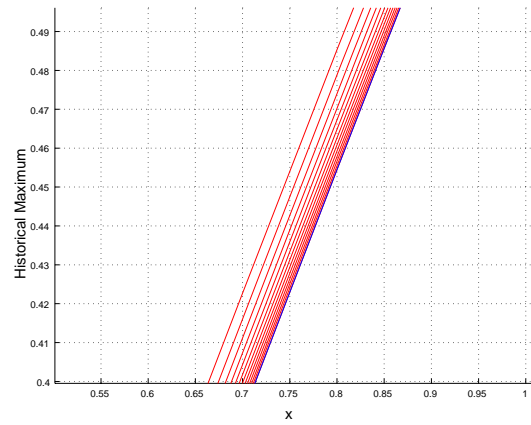


(b) Convergence of $S_{V:m,n}(t)$ to $S_{800}(t)$ where $V = 200, 250, \dots, 800$

Figure 3.1: Survival Function of the First Passage Time of $X_V(t)$
 $(m = \eta_V(0) + V = V \text{ and } n = \eta_V(1) + V)$

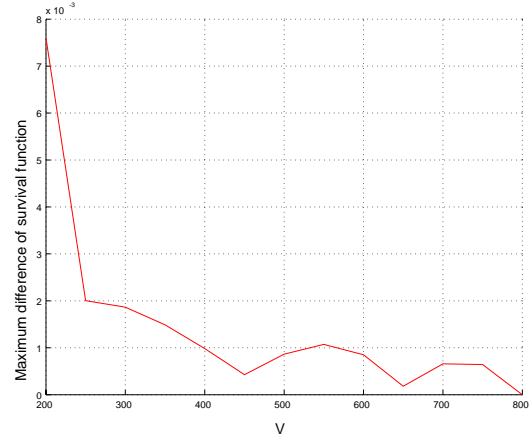
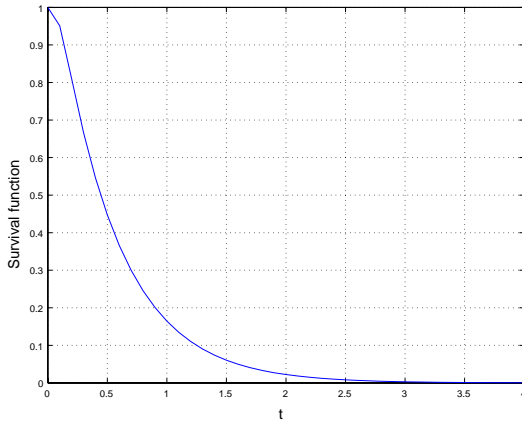


(a) Overview



(b) Enlarged View

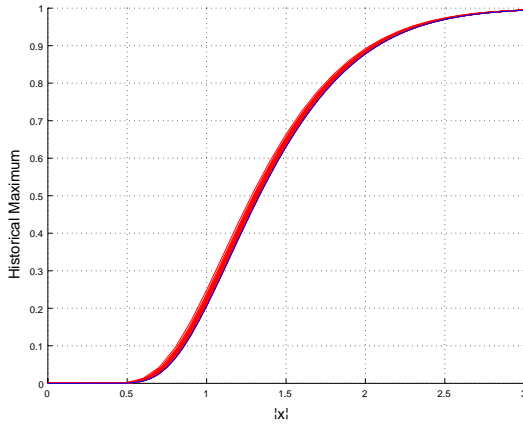
Figure 3.2: Convergence of Distribution Function of Historical Maximum of $X_V(t)$
 $(x_0 = 0 \text{ and } V = 200, \dots, 800)$



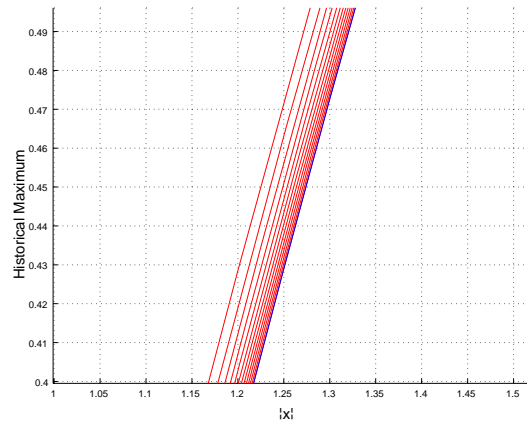
(a) Survival Function $S_{V:m,n}(t)$ with $V = 200$

(b) Convergence of $S_{V:m,n}(t)$ to $S_{800:m,n}(t)$ where $V = 200, 250, \dots, 800$

Figure 4.1: Survival Function of the First Passage Time of $|X_V(t)|$
 $(m = \eta_V(0) + V = V \text{ and } n = \eta_V(1) + V)$



(a) Overview



(b) Enlarged View

Figure 4.2: Convergence of Distribution Function of Historical Maximum of $|X_V(t)|$
 $(x_0 = 0 \text{ and } V = 200, \dots, 800)$

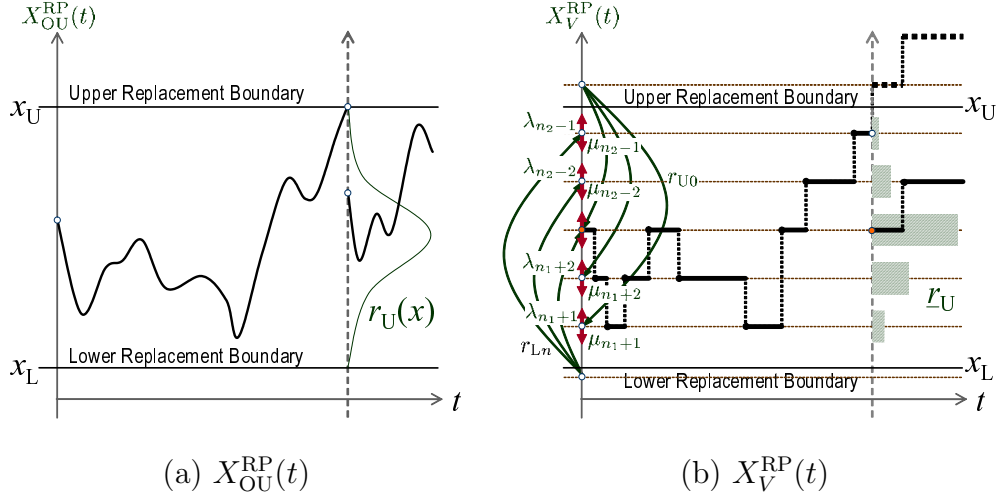


Figure 5.1: Two Processes with Double Replacement Boundaries

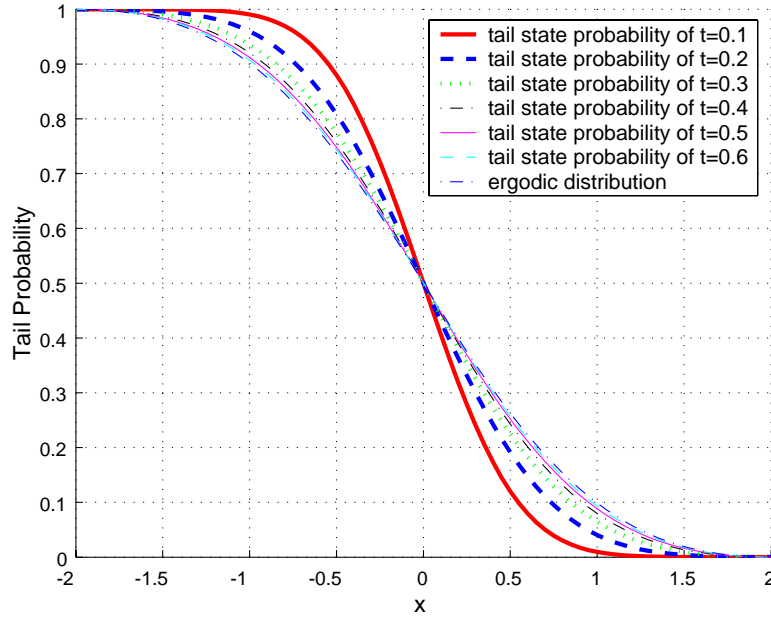


Figure 5.2: Convergence of Tail State Probability with Two Replacement Boundaries
 $(V = 800, x_L = -2, x_U = 2)$

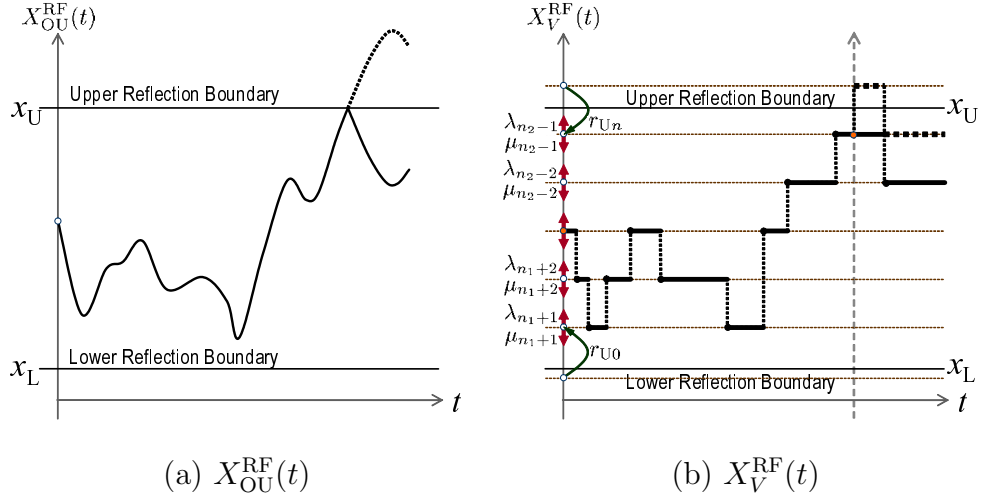


Figure 5.3: Two Processes with Double Reflection Boundaries

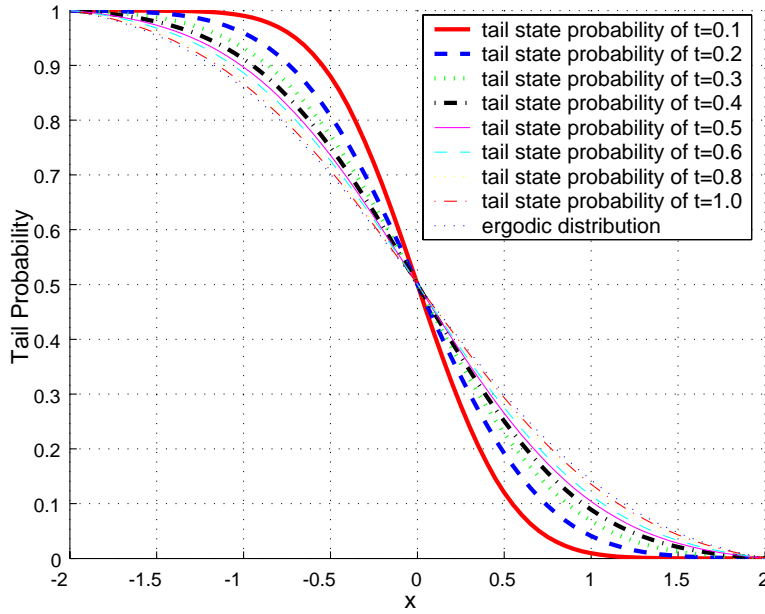
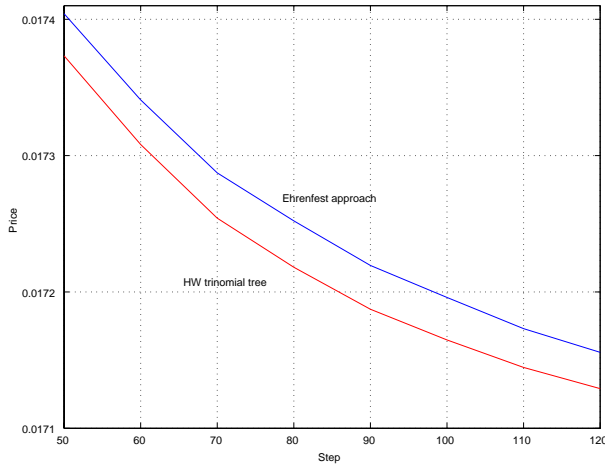
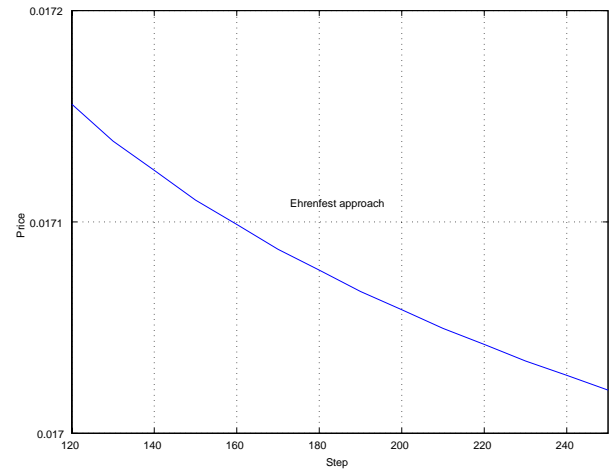


Figure 5.4: Convergence of Tail State Probability with Two Reflection Boundaries
($V = 800$, $x_L = -2$, $x_U = 2$)



(a) $M = 50$ to 120



(b) $M = 120$ to 250

Figure 6.1: Comparison of Up-and-Out Option Prices